Aoyanagi, Kazuki; Tanaka, Hitoshi; Kanayama, Susumu; Fujita, Yutaka

Numerical Simulation of Large-Scale Internal Seiche in Lake Inawashiro

Numerical Simulation of Large-Scale Internal Seiche in Lake Inawashiro

Kazuki Aoyanagi[1], Hitoshi Tanaka[2], Susumu Kanayama[3] and Yutaka Fujita[4]

[1] Graduate Student, Department of Civil Engineering, Tohoku University
6-6-06, Aoba, Sendai, 980-8579, Japan, e-mail: k.aoyanagi@kasen1.civil.tohoku.ac.jp
[2] Professor, Department of Civil Engineering, Tohoku University
6-6-06, Aoba, Sendai, 980-8579, Japan, e-mail: tanaka@tsunami2.civil.tohoku.ac.jp
[3]Senior Research Engineer, PENTA-OCEAN Institute of Technology
1534-1 Yonkusho, Nasushiobara-shi, Tochigi, 329-2746, Japan
e-mail: Susumu.Kanayama@mail.penta-ocean.co.jp
[4] Associate Professor, Department of Civil Engineering, Nihon University
1 Nakagawara, Tokusada, Tamura, Koriyama 963-8642, Japan, fujita@civil.ce.nihon-u.ac.jp

ABSTRACT

Aquatic environments such as rivers, seas, lakes have been drawn a lot of attention in our society due to their close relationship with human beings. Among them, preservation of lakes is very important because of their enclosed characteristics. In this paper, a study on Lake Inawashiro located in Fukushima Prefecture, is described. This lake is well known as the largest acid lake in Japan. The water from the Nagase River pours into the lake from the north is the cause of acid water in the lake. Preservation of water quality is very important because Lake Inawashiro is a valuable aquatic resource. However, water quality changes such as eutrophication and a rise of pH in the lake due to inflow from the surrounding area is now a big concern. Among various hydrodynamic processes, internal seiche can be responsible for causing large oscillation all over the lake, promoting vertical mixing and greatly affecting water quality. Therefore, it is important to investigate the characteristics of internal seiche and its effect to water movement and water quality in the lake. This study is an attempt to reproduce occurrence of large-scale internal seiche in Lake Inawashiro by using a numerical simulation method.

Keywords: Lake Inawashiro, internal seiche, stratification, numerical simulation, field observation

1 INTRODUCTION

In an enclosed water area in a lake, exchange of the water is inherently weak and hence the flow tends to be stagnant. Due to this characteristic in a lake environment, natural purification of water quality progresses slowly in general. Once it is contaminated, therefore, water improvement and maintenance are extremely difficult. Especially, in case of low exchange rate in a lake, the water quality can easily become worse, and the eutrophication is highly concerned. It is well known that due to regulation of factory effluent and sewage improvement, river water quality flowing into a closed water area has been largely improved in comparison with the past. However, water quality improvement in a closed water area has not been readily advanced.

In this paper, a numerical study on Lake Inawashiro is described. Lake Inawashiro is located at the center of Fukushima Prefecture in Japan, extending over Aizuwakamatsu City, Koriyama City, Inawashiro Town and Bandai Town. The location of Lake Inawashiro is shown in Fig.1.

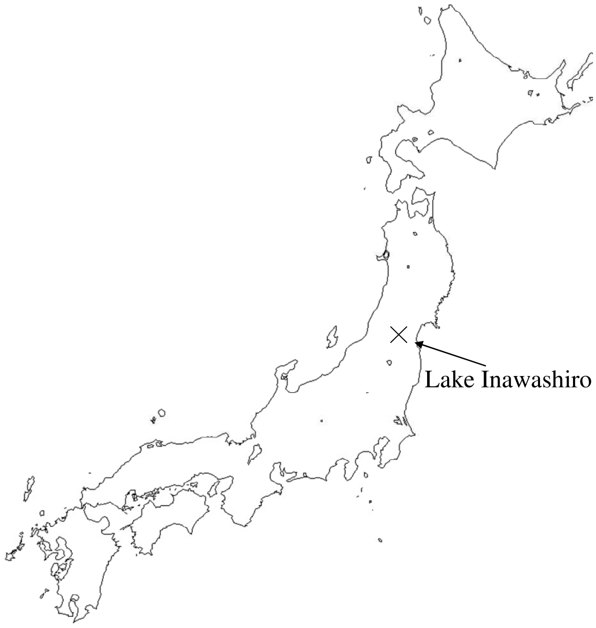

Fig.1 Location of Lake Inawashiro.

The lake is the fourth largest freshwater lake in Japan, which has a perimeter of 55.32km, maximum depth reaches down 93.5m, and the area is $103.9m^2$. This lake has importance role as valuable tourist attractions and aquatic resources in this area. For example, a lot of people visit this lake for bathing in summer, and it is used as water resource for citizen's drinking water.

This lake has shallow depth area in the northern part, and the rest of the part has an inverse-cone shape with the maximum water depth of about 90m. Among 30 rivers flowing into Lake Inawashiro, the Nagase River occupies about 50% of the total discharge inflowing into the lake, and is an acidity river affected by extremely strong acid from one of the tributary streams. Due to acidic river discharge from the Nagase River, Lake Inawashiro is a typical acid lake. Although Lake Inawashiro is an enclosed water area, biological productivity is extremely low, and eutrophication does not advance due to restraint of phytoplankton increase, resulting in good water quality in the lake.

The mechanism of phosphorous removal is flocculation enhanced by acidic Nagase River discharge containing high concentration of iron and silicon (Fujita and Nakamura, 2007). It is reported that deposition of floc can be observed on the entire lake bottom even at the 90m water depth. However, the hydrodynamic mechanism of transport and diffusion of flocculated sediment in the lake is not clarified yet.

Among various hydrodynamic phenomena, an internal seiche can be a one of the important processes that causes large-scale mixing in the lake (Tanaka et al., 2002). Since it is extremely difficult to investigate the mechanism based on field observation because of its large area of the lake, a numerical simulation method is applied in this study for investigating the flow characteristics in the lake.

2 FIELD OBSERVATION DATA

The field data used for model verification in the present study has been obtained by Aoyanagi et al. (2007) from October 18 to October 21, 2000. Figure 2 shows the depth contours in Lake Inawashiro along with observation points of water level, water temperature and wind speed and direction.

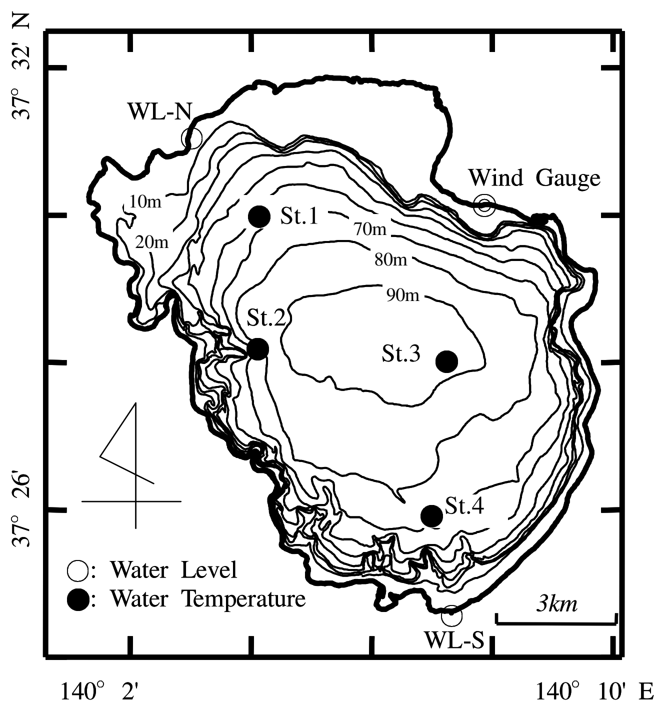

Fig.2 Outline of Lake Inawashiro and observation points of water level, water temperature and wind speed.

A water level gauge was installed at the northern and the southern stations in the lake, WL-N and WL-S as shown in Fig.2. Water temperature was measured using a water thermometer (Stow Away Tidbit, ONSET Computer Corporation) which has an accuracy ±0.2 deg at the maximum. Measurement interval of the water temperature was 10 minutes. Wind velocity was also measured with 10 minutes interval. Direction of the wind was measured based on classification into 16 directions. Since the height of the wind gauge was 4.5m, the measured wind speed is converted into that at the height of 10m using the logarithmic law given by the following equation.

$$U = \frac{u_*}{\kappa} \ln\left(\frac{z}{z_0}\right) \tag{1}$$

where U is the wind velocity, u_* is the friction velocity, κ is the Karman constant, z is the height above the ground and z_0 is the roughness height. In this study, κ=0.4 and z_0=0.001m are employed in Eq.(1), considering grand cover in this area. Converted wind velocity is shown in Fig.3, along with the corresponding wind direction in Fig.4. Furthermore, a histogram of the wind direction is illustrated in Fig.5 to show the predominant wind direction in the study area. Figure 5 indicates that west to northwest direction is most predominant. The wind data shown in Figs.3 and 4 is used in a numerical simulation to estimate wind shear stress acting on the lake water surface.

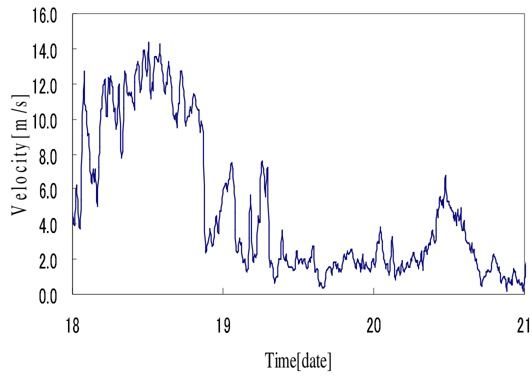

Fig.3 Wind velocity.

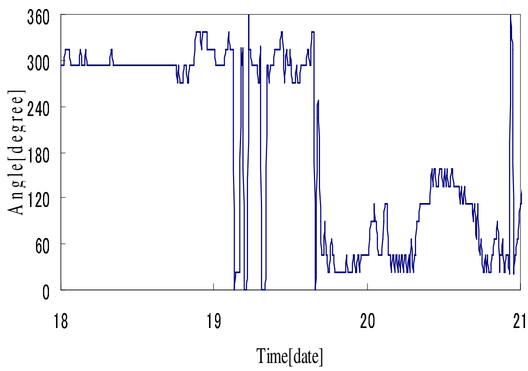

Fig.4 Wind direction.

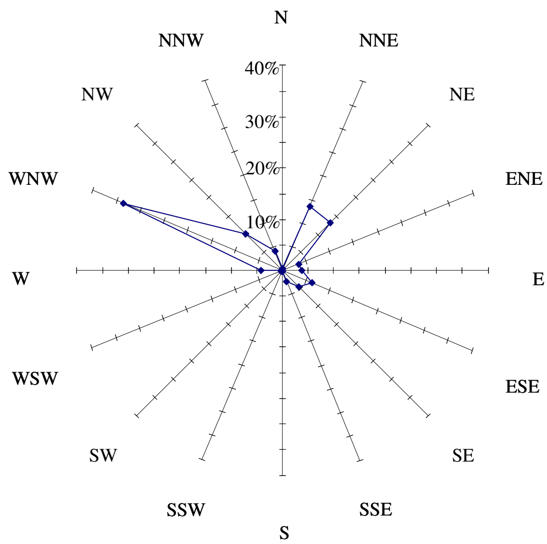

Fig.5 Histogram of wind direction

3. METHOD OF NUMERICAL SIMULATION

3.1 Governing Equations

The hydrodynamic model adopted here is the one based on the hydrostatic pressure approximation and the Boussinesq approximation, and fixed layer divisions in vertical discretization. This model basically follows the procedure introduced by Sato et al. (1993) with addition of baroclinic term to take into account the effect of density gradient. A set of governing equations is required to compute four unknowns, three velocity components and water level. The momentum equations are

$$\frac{\partial u}{\partial t}+u\frac{\partial u}{\partial x}+v\frac{\partial u}{\partial y}+w\frac{\partial u}{\partial z}=-g\frac{\partial \eta}{\partial x}-\frac{g}{\rho_0}\frac{\partial}{\partial x}\int_z^{\eta}\rho' dz+\nu_h\left(\frac{\partial^2 u}{\partial x^2}+\frac{\partial^2 u}{\partial y^2}\right)+\frac{\partial}{\partial z}\left(\nu_v\frac{\partial u}{\partial z}\right) \quad (2)$$

$$\frac{\partial v}{\partial t}+u\frac{\partial v}{\partial x}+v\frac{\partial v}{\partial y}+w\frac{\partial v}{\partial z}=-g\frac{\partial \eta}{\partial y}-\frac{g}{\rho_0}\frac{\partial}{\partial y}\int_z^{\eta}\rho' dz+\nu_h\left(\frac{\partial^2 v}{\partial x^2}+\frac{\partial^2 v}{\partial y^2}\right)+\frac{\partial}{\partial z}\left(\nu_v\frac{\partial v}{\partial z}\right) \quad (3)$$

and the continuity equation is

$$\frac{\partial u}{\partial x}+\frac{\partial v}{\partial y}+\frac{\partial w}{\partial z}=0 \tag{4}$$

where (u,v,w) are flow velocity in the direction of (x,y,z), η is the height of free water surface, g is the gravity, ρ_0 is a constant reference density, $\rho'(x,y,z,t)$ is the local variation from the reference density, and ν_h and ν_v are the eddy viscosity coefficients in horizontal and vertical directions, respectively. Calculation of η is based on depth integration of Eq.(4) with kinematic boundary condition at the free surface to obtain

$$\frac{\partial \eta}{\partial t}+\frac{\partial}{\partial x}\left[\int_{-H}^{\eta} u dz\right]+\frac{\partial}{\partial y}\left[\int_{-H}^{\eta} v dz\right]=0 \tag{5}$$

where H is depth of bottom boundary measured from undisturbed free water surface.

Water density is calculated by using water temperature resulted from solution of the associated advection diffusion equation.

$$\frac{\partial T}{\partial t}+u\frac{\partial T}{\partial x}+v\frac{\partial T}{\partial y}+w\frac{\partial T}{\partial z}=\frac{\partial}{\partial x}\left(\varepsilon_h\frac{\partial T}{\partial x}\right)+\frac{\partial}{\partial y}\left(\varepsilon_h\frac{\partial T}{\partial y}\right)+\frac{\partial}{\partial z}\left(\varepsilon_z\frac{\partial T}{\partial z}\right)+\frac{1}{\rho_0 C_p}\frac{dq}{dz} \tag{6}$$

where T is water temperature, q is heat flux, C_p is specific heat of water, ε_h and ε_v are the eddy viscosity coefficients in horizontal and vertical directions, respectively.

3.2 Calculation conditions

In the present numerical computation, *x-y* coordinates system is used in the direction of east-west and north-south. The mesh size is $\Delta x = \Delta y = 100$m, and the time increment Δt is determined to be 1s to satisfy the CFL (Courant-Friedrichs-Levy) condition. The grid spacing in the vertical direction changes from finer to courser from the surface to the bottom. The eddy viscosity in the vertical and horizontal directions is assumed to be 0.001m^2/s. More detailed description of the model and numerical solution method can be found in Purwanto et al. (2006).

4 CALCULATION RESULTS AND DISCUSSIONS

4.1 Water temperature variation

In Figs. 6 to 13, the water temperature variations from field observation and from numerical simulation are compared for the period from October 18 to October 21. It is seen that large-scale internal seiche occurred by a strong wind on 18th, and afterwards, continuous oscillation of the contours can be observed for a few days. Especially, the amplitude of oscillation is larger at St.1 and St.2. From the difference of the amplitude among the measuring stations, it is concluded that the node of oscillation is located near the center of the lake, whereas the anti-node is formed at the northern and southern end of the lake. The present numerical simulation reproduces this phenomenon quite well at all measuring stations, including spatial difference of the oscillation amplitude.

Next, spectral analysis is employed to make a quantitative evaluation of the model reproductivity from the viewpoint of oscillation period of temperature. Figures 14 to 17 are spectrum of water temperature at 25m depth from the measurement and from the numerical modelling at each station, in which f is the frequency and $P(f)$ is the power spectrum. In addition, ‘obs’ in a figure shows an analysis result from the field observation, whereas ‘sim’ denotes an analysis result from the present simulation. From these figures, it is seen that the predominant periods of water temperature variation is almost 18.0 hours, and is almost same among each stations. In Figs.14 and 15, the computation underestimates the period of the peak, while good agreement can be seen at St.3. At St.4, the predominant period is not so clearly visible.

The period of oscillation of internal seiche in a lake with two-layer stratification can be estimated from the following theoretical equation.

$$T_i = {}^{2L}\!\big/_{c_i} \tag{7}$$

where T_i is period of internal seiche L is the length of a lake and c_i is the celerity of internal Kelvin wave. In Eq.(7), the celerity of internal wave c_i is given by Eq.(8).

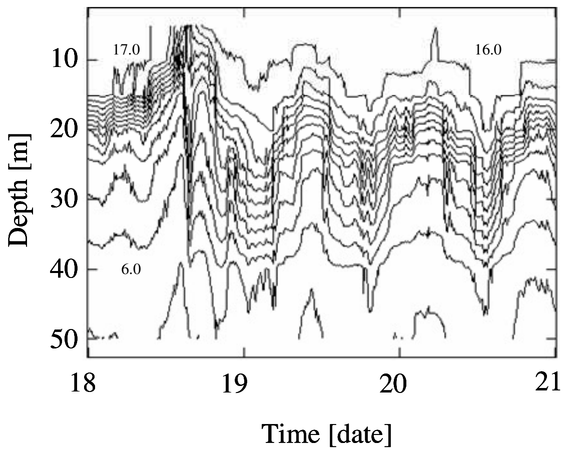

Fig.6 Field observation result of water temperature (St.1)

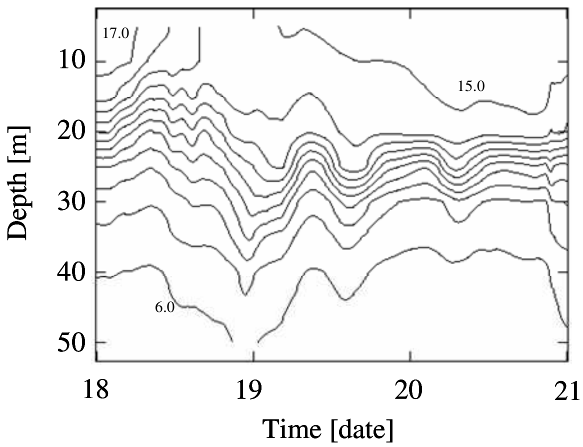

Fig.7 Numerical simulation result of water temperature (St.1)

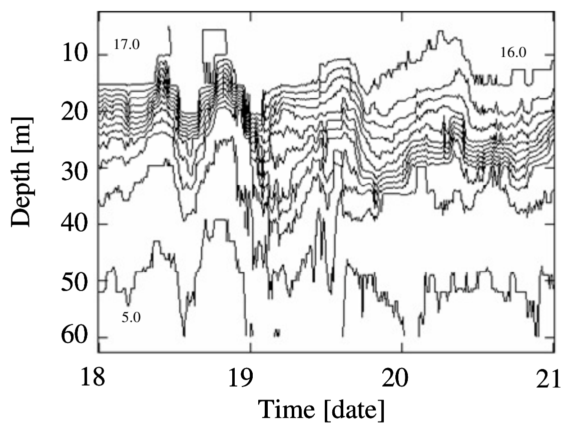

Fig.8 Field observation result of water temperature (St.2)

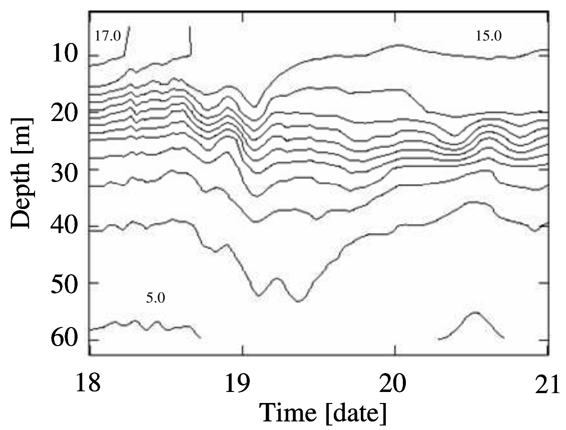

Fig.9 Numerical simulation result of water temperature (St.2)

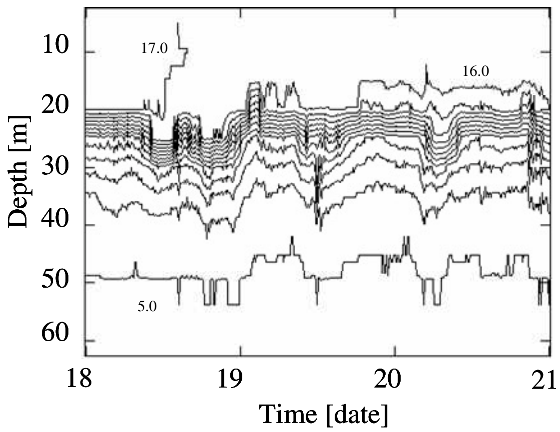

Fig.10 Field observation result of water temperature (St.3)

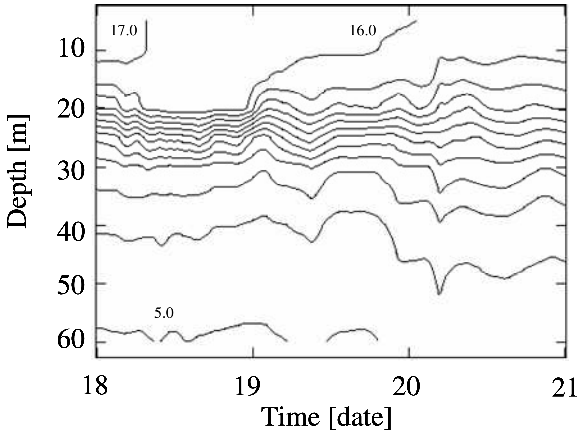

Fig.11 Numerical simulation result of water temperature (St.3)

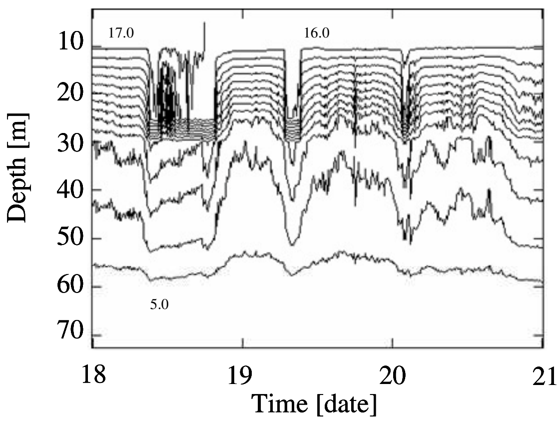

Fig.12 Field observation result of water temperature (St.4)

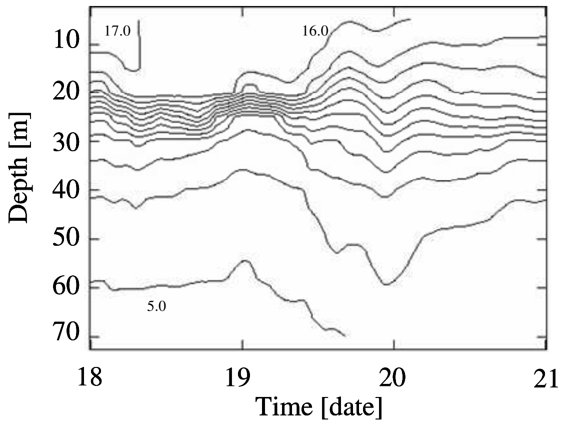

Fig.13 Numerical simulation result of water temperature (St.4)

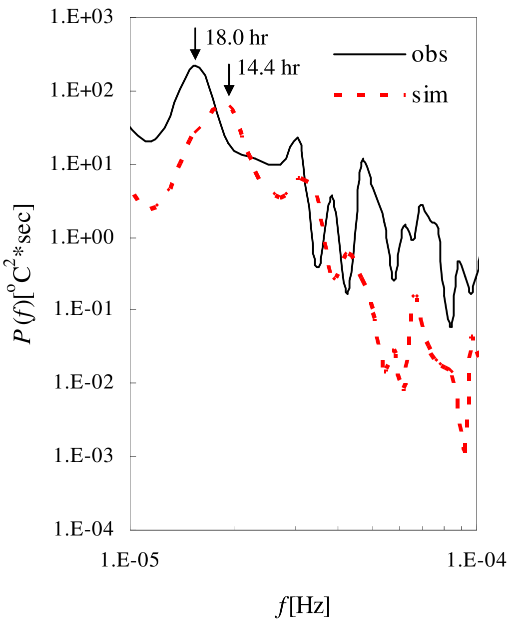

Fig.14 Spectrum of water temperature at 25depth (St.1)

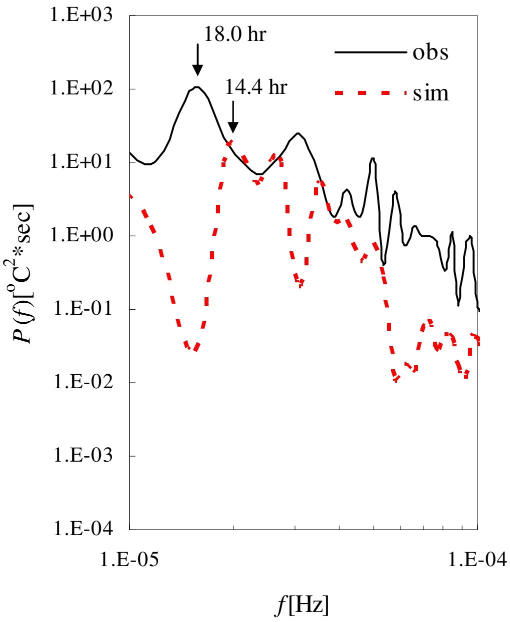

Fig.15 Spectrum of water temperature at 25depth (St.2)

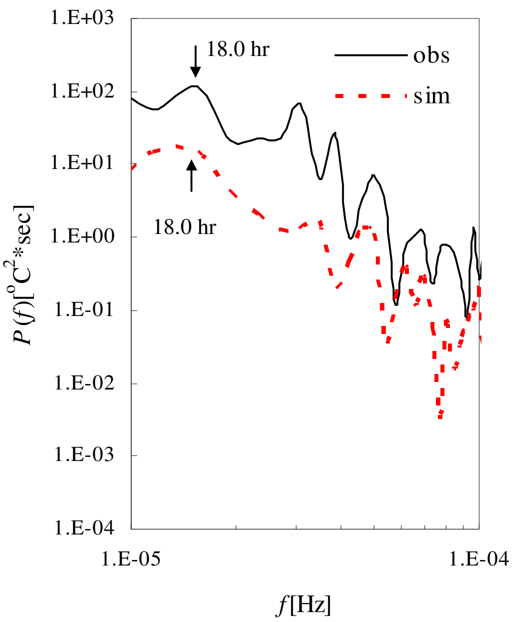

Fig.16 Spectrum of water temperature at 25depth (St.3)

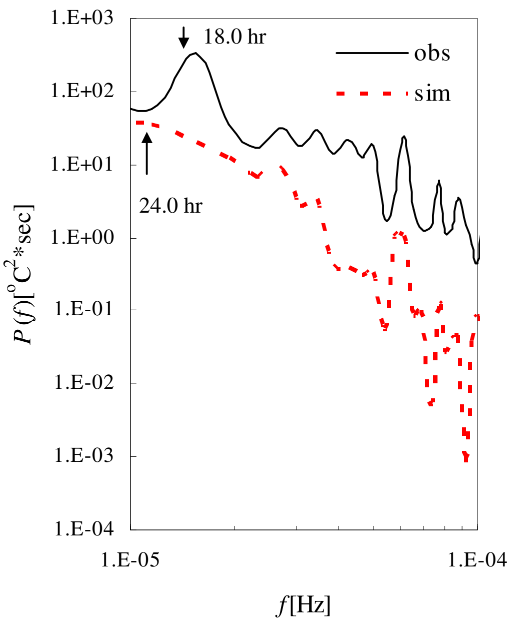

Fig.17 Spectrum of water temperature at 25depth (St.4)

$$c_i = \sqrt{\frac{\varepsilon g h_1 h_2}{h_1 + h_2}} \tag{8}$$

where h_1 and h_2 are the thickness of upper and lower layers, respectively, and ε is the relative density difference between upper and lower layers defined by,

$$\varepsilon = \frac{\rho_2 - \rho_1}{\rho_1} \tag{9}$$

where ρ_1 and ρ_1 are the water density of upper and lower layers, respectively. Quantities used for the calculation by Eq.(7) and the calculation result are summarized in Table 1. It is seen that the computed period in Table 1 shows satisfactory agreement with the measurement in Figs.14, 15, 16 and 17.

Table 1 Quantities used in Eq.(7) and computed period of internal seiche.

L	ε	h_1	h_2	T_i
11,000m	0.000803	20m	40m	18.9hr

4.2 Water level variation

Similar to internal oscillation of thermocline described above, water surface oscillation can also be observed in the lake. Figure 18 shows comparison between observation at WL-N and computation at St.1 located in northern area of the lake, while Fig.19 denotes comparison of water level at WL-S (observation) and St.4 (computation) shown in Fig.2. It is seen that the computation gives underestimated water level change, although overall shape of the time-variation of water level in response to wind speed can be predicted by the numerical model.

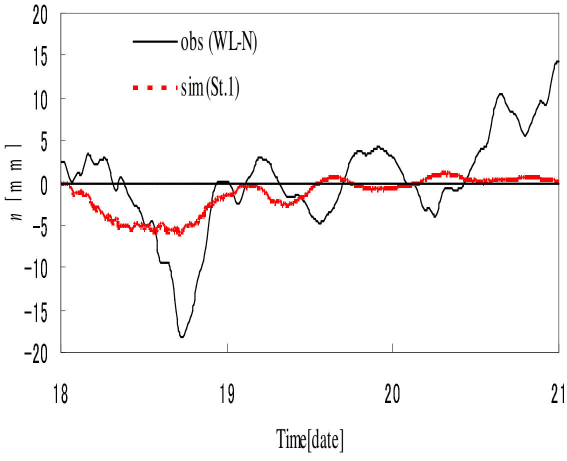

Fig. 18 Water level (WL-N and St.1)

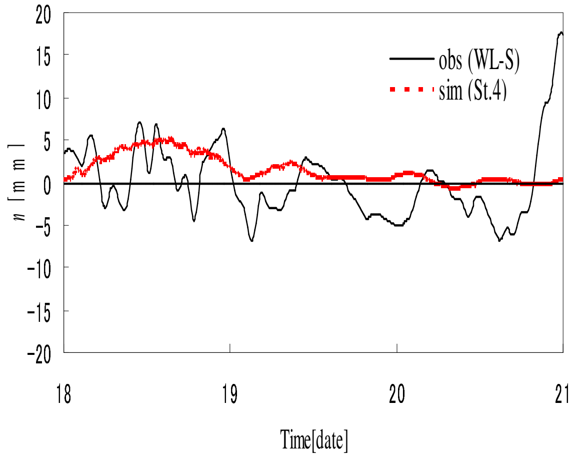

Fig. 19 Water level (WL-S and St.4)

5 CONCLUSION

In this study, a field observation data of the water temperature and water level in Lake Inawashiro in Fukushima Prefecture was numerically simulated for a period when the stratification was weak in autumn. As a result, water temperature change in the lake is reproduced well by the numerical simulation. Especially, the occurrence of large-scale internal seiche is successfully simulated. The influence of the large-scale seiche on water quality change will be investigated in future studies.

ACKNOWLEDGMENTS

The authors gratefully acknowledge the financial support as grant for "Academic Frontier Project" from the Ministry of Education, Culture, Sports, Science, and Technology, Japan.

REFERENCES

Aoyanagi, K., Tanaka, H. and Fujita, Y. (2007), Field investigation of internal seiche in Lake Inawashiro, *Proceedings of International Conference on Violent Flow*. (CD-ROM)

Fujita, Y. and Nakamura, M. (2007), Effect of floc produced in acid Nagase River on phosphors removal in Lake Inawashiro, *Journal of Japan Society on Water Environment*, Vol.30, No.4, pp.197-203. (in Japanese)

Fujita, Y. and Nakamura, M. (2007) Production Mechanism of Floc Produced in Acidic Nagase River Concerning Phosphorus Removal in Lake Inawashiro, *Journal of Japan Society on Water Environment*, Vol.30, No.4, pp.205-212. (in Japanese)

Purwanto, B.S., Tanaka, H., Kanayama, S., Takasaki, M. and Yamaji, H. (2006), Transport mechanism in Nagatsura-ura Lagoon, *Proceedings of 2nd International Conference on Estuaries and Coasts,* pp.615-622.

Sato, K., Matsuoka, M. and Kobayashi, K. (1993) Efficient calculation method of 3-D tidal current, *Proceedings of Coastal Engineering JSCE*, Vol.40, pp.221-225 (in Japanese)
Tanaka, H., Fujita, Y. and Yamaji, H. (2002), Visualization of large-scale internal seiche in Lake Inawashiro, *Proceedings of the 10th International Symposium on Flow Visualization*. (CD-ROM)